

EXPERIMENTAL – NUMERICAL ANALYSIS OF STRESS STATE IN FRONT OF THE CRACK TIP OF MODIFIED AND UNMODIFIED G17CrMo5-5 CAST STEEL BY RARE EARTH METALS IN A BRITTLE-DUCTILE TRANSITION REGION

In the paper presented experimental data and numerical analysis of stress distribution in front of the crack of two melts of low-alloy G17CrMo5-5 cast steel-modified (M) by rare earth metals and original, unmodified (UM) in the temperature range, according to the brittle-ductile transition region. Experimental tests include determination of the tensile properties and fracture toughness characteristics for the UM and M cast steel. Numerical analysis includes determination of stress distribution in front of the crack at the initial moment of the crack extension. In the numerical computations, experimentally tested specimens SEN(B) were modeled. The true stress–strain curves for the UM and M cast steel were used in the calculation. It was shown that the maximum of the opening stresses at the initial moment of the crack extension occurs in the axis of the specimens and reaches similar level of about $3.5\sigma_0$ for both UM and M cast steel. However, the length of the critical distance, measured for stress level equal $3\sigma_0$, is great for the M in comparison to the UM cast steel. Also was shown that the UM cast steel increased the level of the stress state triaxiality parameters that resulted in a decrease of fracture toughness.

Keywords: fracture toughness in a brittle-to-ductile transition region, stress distributions in front of the crack, cast steel, modification by rare earth metals

1. Introduction

Low-alloy cast steels elements are widely used in different branches of economy. One of the main problems observed during using of these elements is occurring a sudden destruction. In several studies were received wide scatter intervals and low levels of impact energy data for cast steels [1-3]. The modification of cast steels by rare earth metals (REM) leads to an increase of mechanical properties, caused by changes of the shape and distribution of nonmetallic inclusions [1-6]. For low-alloy G17CrMo5-5 cast steel, especially a significant increase was obtained for the fracture toughness characteristics.

According to the local approach to fracture, the fracture process begins if the level of stresses (or strains) in front of the crack, exceeds the critical value on the critical distance [7-11]. The modified Ritchie-Knott-Rice's criterion for the beginning of fracture process determines a level of the opening stress that must be exceeded on the critical distance [12,13]. In the presented study, authors concentrated on the numerical method calculations of stress distributions and triaxiality parameters of the stress state in front of the crack, for the modified (M) and unmodified (UM) cast steel G17CrMo5-5, in the brittle-to-ductile transition region. Based on the distributions of the opening stress, the critical distances will be estimated. The stress distribution results will be compared with data of an average size and dispersion of non-metallic inclusions for different temperatures.

2. Tested material and experimental procedures

The chemical composition of G17CrMo5-5 cast carbon steel received from the series of industrial melts that are: 0.17% C, 0.4% Si, 0.6% Mn, 1.2% Cr, 0.53% Mo, 0.1% Ni, 0.034% Al, 0.012% S, 0.018% P. It is in accordance with the EN-10213-2:1999 standard. The difference between the two alloys, based on a modification of one of them with the addition of rare earth metals (REM), with the composition of 49.8% Ce, 21.8% La, 17.1% Nd, 5.5% Pr, 5.35% introduced in the form of mischmetals [3]. Heat treatment after casting included normalizing – 940°C, 1 hour and tempering – 710°C, 2 hours.

In experimental tests carried out on the specimens made of G17CrMo5-5 cast steel in its original and modified state, determined fracture toughness characteristics and material fracture toughness in the region of ductile-to-brittle transition temperature from 60°C to 20°C. In order to obtain negative temperatures, tests were carried out in a thermal chamber in the environment of nitrogen vapors. The temperature was measured with an accuracy of $\pm 0.1^\circ\text{C}$ by a thermocouple mounted directly on the tested specimen. Experimental studies carried out on testing machines equipped with an automated control and data recording systems. On the basis of data recorded during a uniaxial tensile test on quintuple round specimens of 5 mm diameter were determined standard fracture toughness characteristics and true stress-strain dependencies (Fig. 1, Tab. 1), that were used to determine local stresses in front of the crack tip.

* KIELCE UNIVERSITY OF TECHNOLOGY, 7th TYSIĄCLECIA P.P. AV. 25-314 KIELCE, POLAND

Corresponding author: kasinska@tu.kielce.pl

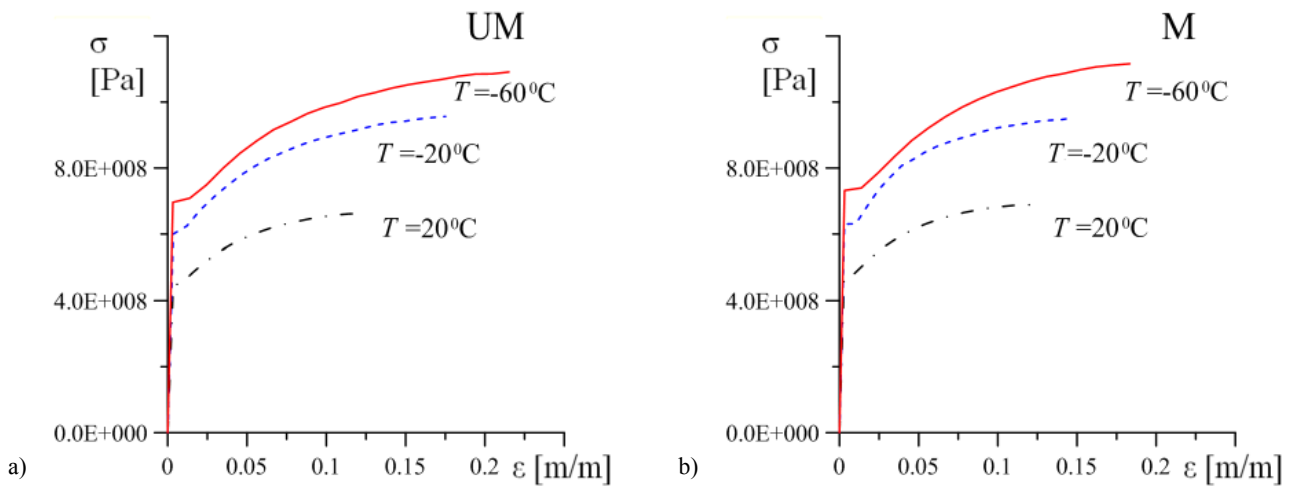


Fig. 1. The true stress-strain curves for the unmodified (a) and modified (b) G17CrMo5-5 cast steel

In order to determine characteristics of fracture toughness critical values, tests were carried out on standard single edge notch in bending, SEN(B), specimens of 12 mm thickness, according to ASTM methodology [14-16]. The results of temperature fracture toughness dependencies show a great positive influence of REM modification on G17CrMo5-5 cast steel. Characteristic temperature of ductile-brittle transition temperature T_0 , for the M cast steel is lower of about 50°C compared to the UM. Fractographic tests of breakthrough of SEN(B) specimens made of the UM and M cast steel showed significant differences in a morphology of the growth of subcritical cracks, and in a creation of a stretch zone width (SZW) in the fatigue crack tip (Fig. 2) [17]. On the basis of accurate SZW measurements made on SEN(B) specimens breakthroughs, were determined values of fracture toughness at the moment of crack ini-

tiation, J_i . Between the values of fracture toughness J_{IC} and J_i , were observed differences, level of which grows with the growth of a ductile fracture participation in a crack growth (Tab. 1) [17]. The observed difference is explained by different moment of extension of the subcritical crack growth during fracture, in which the value of J_i or J_{IC} is determined. The value of J_i corresponds to the moment of subcritical crack growth initiation, while J_{IC} value corresponds to fracture toughness for an average extension of the subcritical crack $\Delta a = 0.2$ mm. In the case of a completely ductile subcritical crack propagation mechanism, the difference between the values J_i and J_{IC} is significant. Along with decreasing the length of ductile extension below $\Delta a < 0.2$ mm, the difference between the values J_i and J_{IC} reduces. For the case of a subcritical crack growth since the moment of initiation by the brittle mechanism, the level of J_i and J_{IC} values is comparable.

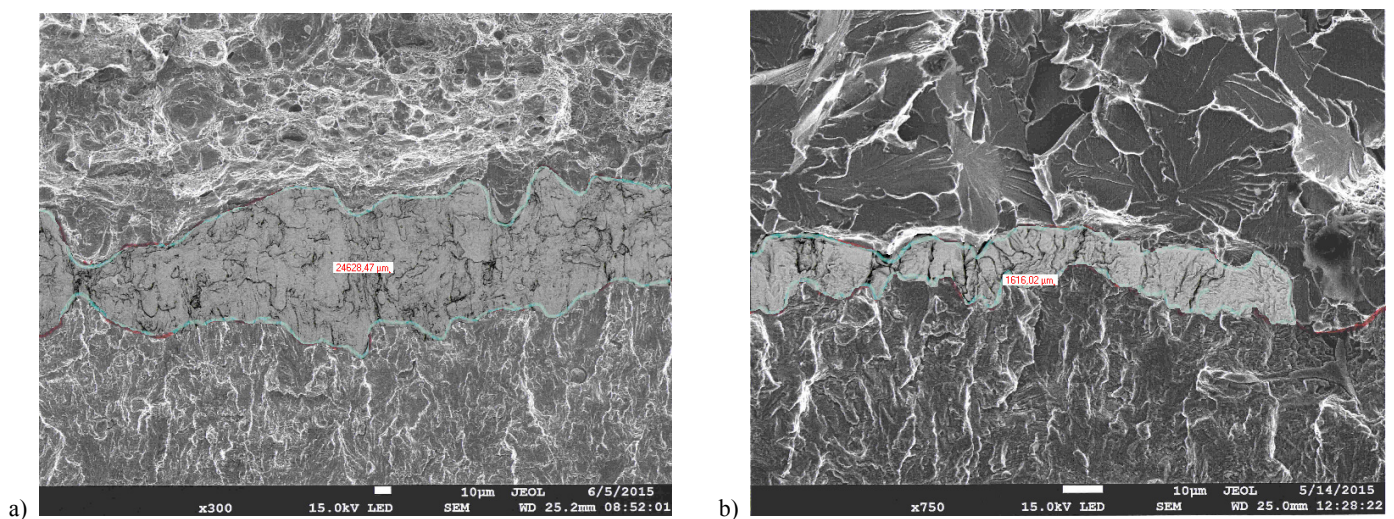


Fig. 2. The morphology of fracture surface in the top of crack-the SZW and crack propagate aria for 20°C (a) and - 60°C (b) in the modified G17CrMo5-5 cast steel

Quantitative microstructural tests showed a series of positive changes in the microstructure of G17CrMo5-5 cast steel as a result of REM modification: the size of ferrite grains reduces,

the size of inclusions particles reduces and their shape changes from irregular to spherical.

3. Numerical studies

Numerical model. For numerical calculations were used experimental results obtained on SEN(B) specimens. Because of the existing symmetry modeled a quarter of the specimen (Fig. 3). The length of the crack is taken as the average crack length measured with a laboratory microscope. The specimen was divided into 10 layers, with a density in the direction of a free surface, due to the higher intensity of stress components changes at a side surface of the specimen. The arched region of a crack tip with a radius of about 4 mm divided into 16 equal parts, and in the radial direction divided into 60 parts. Finite element mesh sizes decreased in the direction of the crack tip. Crack tip was modeled in the form of a quarter of an arch with a radius equal to 10 μm , therefore was 2400 times smaller than the width of the specimen. In calculations used 20 nodal three-dimensional finite elements. Load was applied by means of a displacement of a loading roll to the moment corresponding to the crack initiation. The moment of initiation was determined on the basis of the analysis of a 'force-specimen deflection' load curves. In the case of the occurrence of brittle fracture, the initiation moment corresponds to the moment of specimen destruction. During a ductile growth of the subcritical fracture, the critical moment was calculated from the J_i value, determined by measuring the width of stretch zone. The specimen material was modeled by means of dependencies of the true 'stress-strain' obtained on the basis of a uniaxial tensile test on specimens of the M or UM cast steel and for the appropriate test temperature (Fig. 1). Calculations assume a model of large deformations. Modeling of the specimen and calculations were carried out in program Adina 8.7.

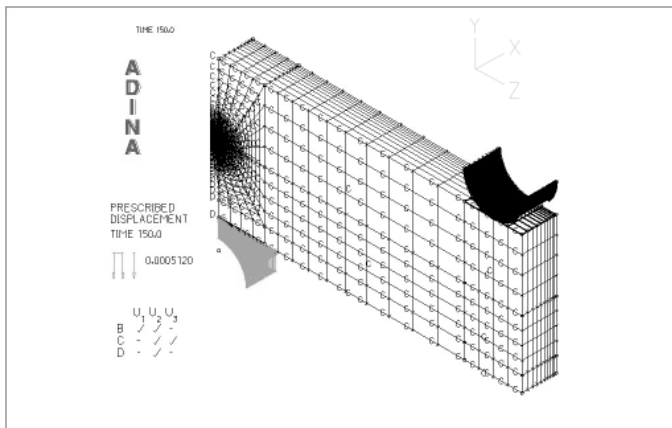


Fig. 3. The SEN(B) specimen model and mesh used in numerical calculation

Results of numerical calculations. The components of opening stresses σ_{zz} , stresses in the direction of the crack tip growth σ_{xx} and stresses in the direction of thickness σ_{yy} , in front of the crack tip, for the temperatures +20°C, -20°C, -60°C, in the central layer of the specimens made of the M and UM cast steel were calculated. Opening stresses distributions σ_{zz} for different temperatures were shown in the Figure 4. Distributions of stress components σ_{xx} , and σ_{yy} maintaining the similar shape, achieve

lower values. Exemplary plots of stresses distributions σ_{xx} , and σ_{yy} for the tests temperature -20°C were shown in the Figure 5. The results of the calculations lead to the conclusion, that for a subcritical crack initiation in the modified material, higher level of stresses components is needed, than in the unmodified. Crack initiation in the modified cast steel at each temperature requires a greater critical length of section, on which stresses exceed the critical level, than in the unmodified. Decrease of temperature leads to the growth of a level of stresses necessary to the crack initiation, while the critical length of section reduces.

Stress distributions similar to those presented in the figures 4 and 5 were obtained at each of ten layers, which enabled to determine distributions of stress components through the specimen thickness. Exemplary distributions σ_{zz} and σ_{xx} through thickness for the specimens of the M and UM material shown in the figures 6 and 7. High values of stresses in front of the crack remain along 70-90% of the inner part through the specimen thickness. Decrease of temperature results in the growth of stresses along the whole crack front and in the increase of width, on which occurs a high level of stresses.

Aptitude material to brittle fracture determines a triaxiality factor of stress state in crack tip. It was proposed several forms for triaxiality factor of stress state [21]:

$$3R = \frac{\sigma_{11} + \sigma_{22} + \sigma_{33}}{3\sigma_0} \quad [9] \quad (1)$$

$$3R_e = \frac{\sigma_{11} + \sigma_{22} + \sigma_{33}}{3\sigma_e} \quad [22] \quad (2)$$

$$T_Z = \frac{\sigma_{33}}{\sigma_{11} + \sigma_{22}} \quad [23] \quad (3)$$

In the equations (1-3): $\sigma_{11} = \sigma_{zz}$, $\sigma_{22} = \sigma_{xx}$, $\sigma_{33} = \sigma_{yy}$; σ_0 is the yield stress; σ_e is the effective stress according to Huber-von Mises.

Distributions of triaxiality factor stress state $3R$ along the crack front for the analyzed specimens are shown in the figure 8 and weighted average values of the $3R$ parameter are placed in the Table 1. The $3R$ values grow along with temperature decrease. At temperatures +20°C and -20°C for the specimens of UM cast steel, where was observed brittle mechanism of crack propagation, obtained higher levels of the $3R$ factor, than for the M specimens, where the crack tip grew according to the ductile mechanism. But for test temperature of -60°C, where for the both kinds of cast steel UM and M registered brittle fracture, were obtained comparable values of the $3R$ factor.

4. Results analysis

The experimental tests and numerical analysis revealed a significant, positive influence of REM modification of the G17CrMo5-5 cast steel. As a result of the modification obtained a growth of strength and fracture toughness characteristics [3]. Namely, a significant increase was recorded for the fracture toughness characteristics. On the basis of the numerical analysis

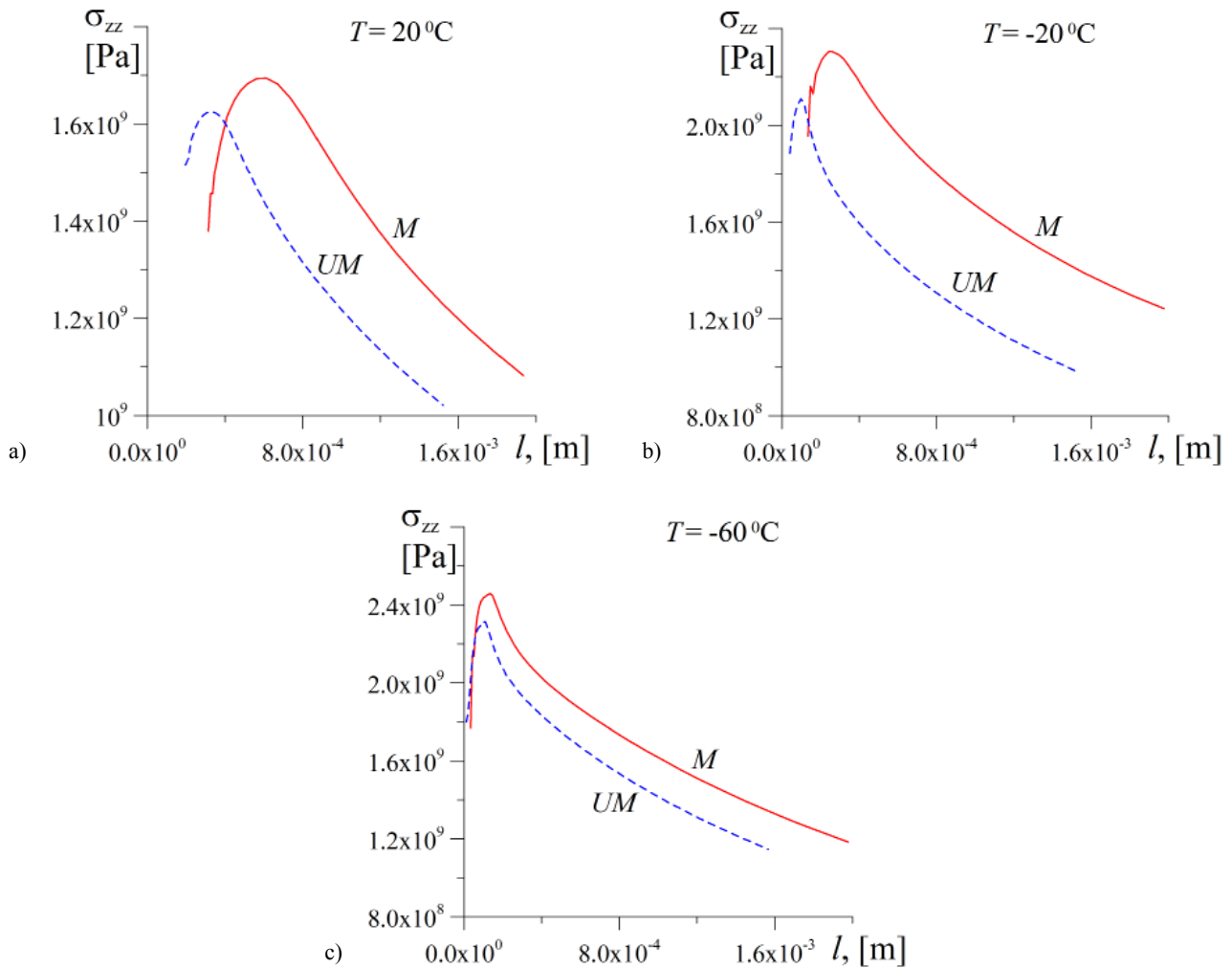


Fig. 4. The opening stress distributions σ_{zz} for the UM and M of G17CrMo5-5 cast steel at test temperature 20°C (a), -20°C (b) and -60°C (c)

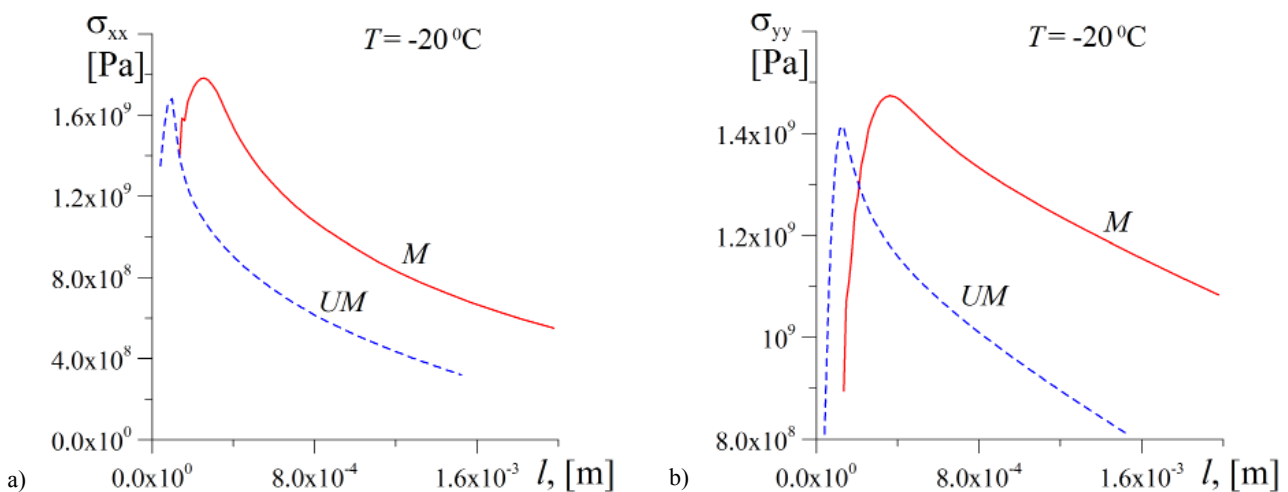


Fig. 5. The distributions of the σ_{xx} (a) and σ_{yy} (b) stress for the UM and M of G17CrMo5-5 cast steel at test temperature -20°C

of the fracture process carried out in the paper, obtained some values that allow to explain peculiarities of development of the cracking process in the UM and M cast steel.

According to the local approach to fracture, the initiation of the subcritical crack growth will exist, if the level of stresses and/or strains achieves a higher level than the critical, on some

critical length of section [7-11]. In the local approach to fracture, proposed by Ritchie, Knott and Rice (RKR), it is assumed that the fracture process is possible if the level of the opening stresses σ_{zz} exceeds the critical value. Modification of this criterion performed by Neimitz et al. [12], through to assuming large finite strains, allows to calculate length of the critical section (Fig. 9).

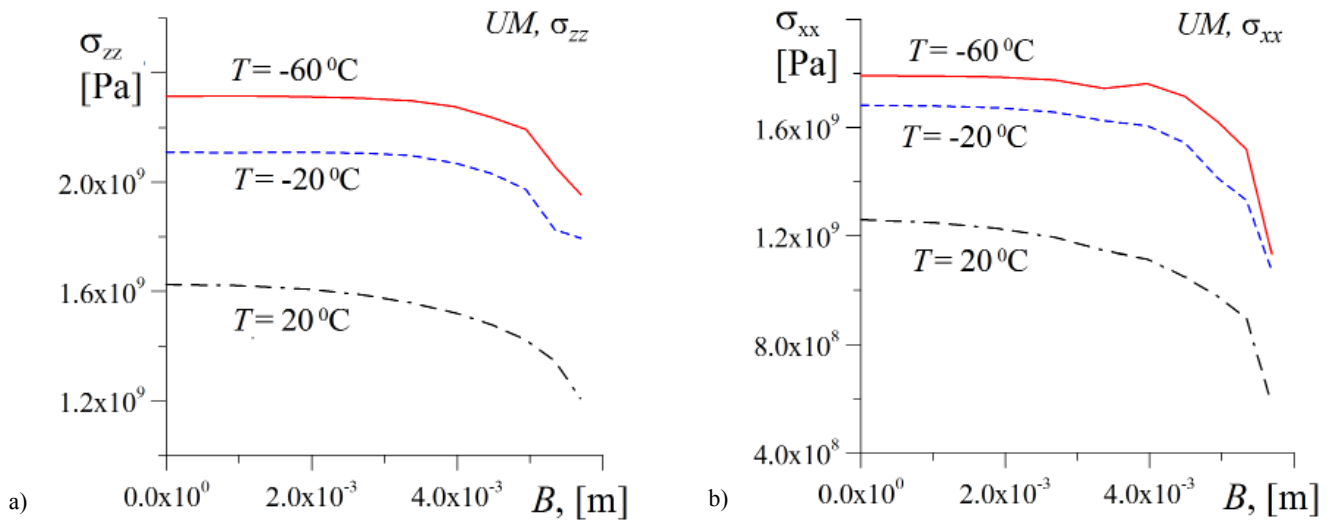


Fig. 6. The opening stress distributions σ_{zz} (a) and stress distributions σ_{xx} (b) in thickness direction for the UM of G17CrMo5-5 cast steel at various temperatures

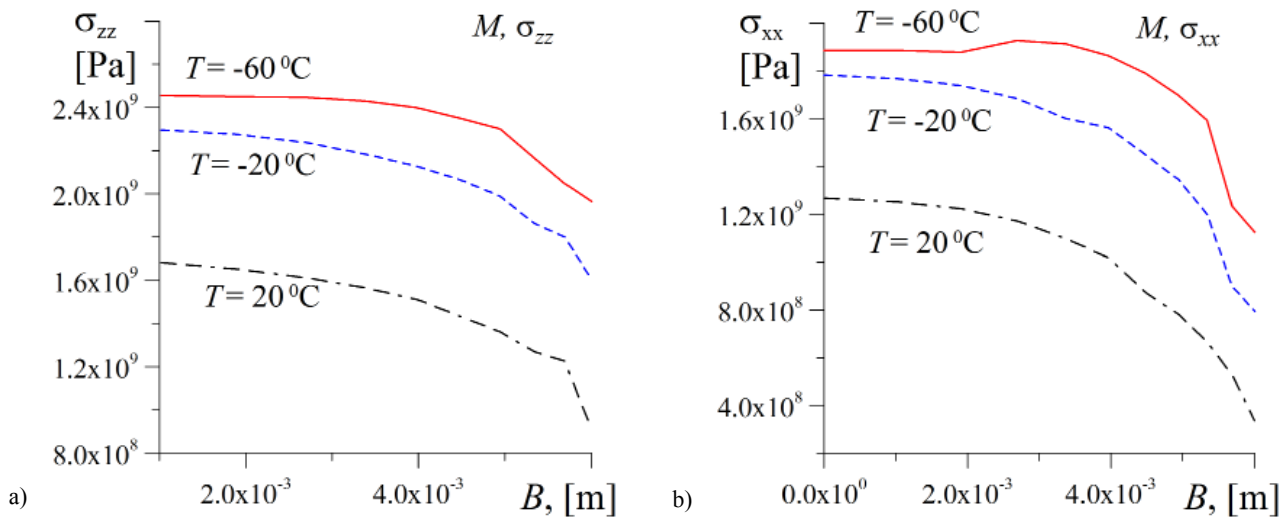


Fig. 7. The opening stress distributions σ_{zz} (a) and stress distributions σ_{xx} (b) in thickness direction for the M of G17CrMo5-5 cast steel at various temperatures

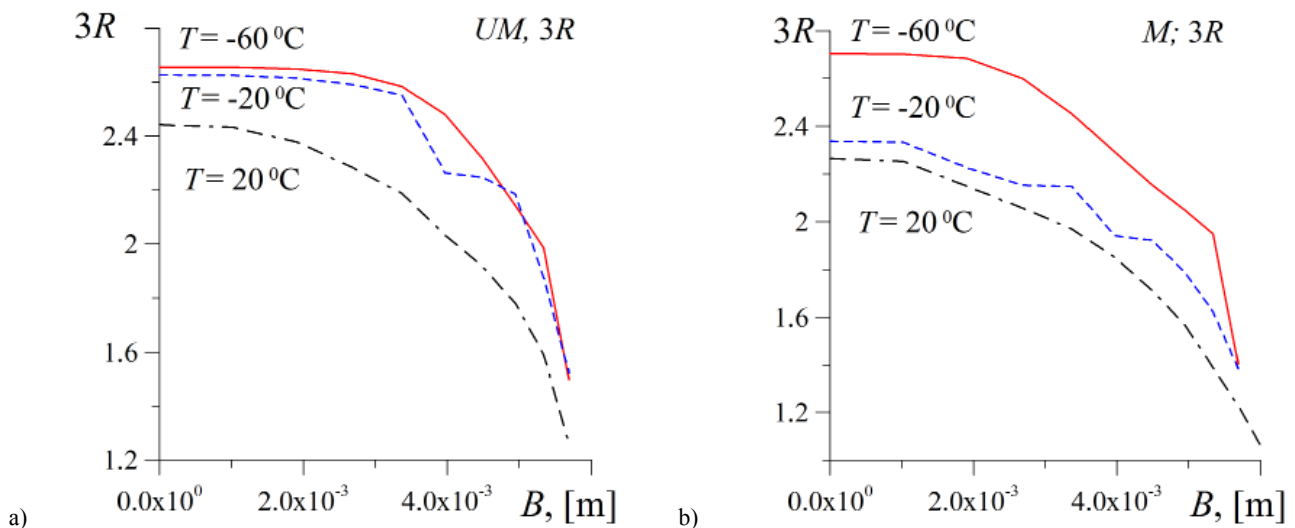


Fig. 8. The 3R parameter distributions in thickness direction for the UM (a) and M (b) of G17CrMo5-5 cast steel at various temperatures

As a critical level of stresses assumed the value of stresses equal $3\sigma_0$, proposed in the RKR criterion and used in Neimitz et al. papers. Values of the opening stresses σ_{zz} are higher than $3\sigma_0$ (Tab. 1). Lengths of the r_c critical section determined on the basis of distributions of the opening stresses σ_{zz} and $\sigma_C = 3\sigma_0$ for proper temperatures (Tab. 1).

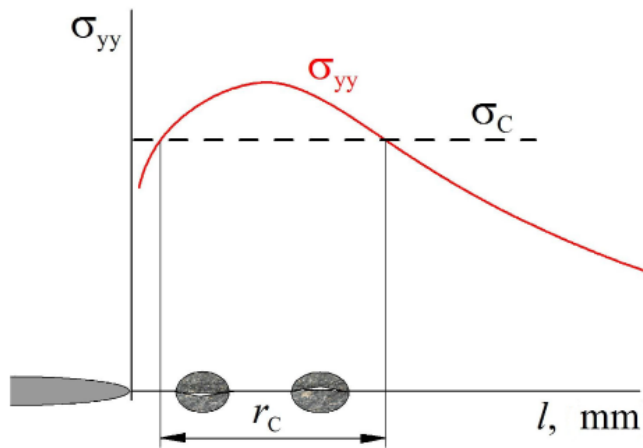


Fig. 9. The scheme of fracture analysis according to the modified RKR criterion

Length of the critical section decreases with a reduction of temperature and a decrease of fracture toughness values. At the same time, with temperature reduction, increases the level of σ_{zz} opening stresses. Growth of the σ_{zz} opening stresses means, that fracture may initiate on the particles of inclusions of smaller sizes, d_w , which occur in the material with a greater frequency [13-18], and this leads to the reduction of critical section length r_c . In the modified cast steel occur particles with a smaller frequency ρ and of smaller sizes d_w , which require a higher level of the opening stresses σ_{zz} on a longer critical section, so the crack initiation takes place at a higher level of J integral. The microstructure of M cast steel consists of finer grains D_z , what is an additional factor of the growth of strength and fracture toughness.

A sensitive indicator of a material tendency to fracture is a factor of triaxiality stress state $3R$. With temperature reduction, the value of a $3R$ factor for the UM and M cast steel increases, while fracture toughness decreases. For the UM cast steel, the values of $3R$ are higher than for the M, which means that in the UM material fracture will occur at lower levels of fracture toughness characteristics.

TABLE 1

Strength and fracture toughness characteristics for UM and M G17CrMo5-5 cast steel

	T , °C	σ_0 , [MPa]	J_{IP} , [kJ/m]	J_{IC} , [kJ/m]	max σ_{zz} , [MPa]	σ_{zz}/σ_0	r_c , [mm]	$3R$	D_z [mm]	d_w , [mm]	ρ [n/mm ²]
UM	20	445	139	246.2	1625	3.65	630	2.16	34.8	3.13	1969
	-20	610	38	38.3	2100	3.44	180	2.42			
	-60	680	34	26.1	2312	3.40	185	2.47			
M	20	470	211	314.5	1695	3.61	805	1.97	23.7	1.78	1128
	-20	647	125	326.3	2305	3.56	475	2.09			
	-60	710	53	53.1	2458	3.46	260	2.43			

Acknowledgments

Financial support of the Polish MSHE contracts 01.0.08.00/2.01.01.01.0035 and 01.0.08.00/2.01.01.02.0016 and NCTA contract PBS1/B5/13/2012 is gratefully acknowledged.

Figure 2 made by Piotr Furmańczyk. Sincere thanks for sharing these photographs.

REFERENCES

- [1] Long-Mei Wang, et al., Study of application of rare elements in advanced low alloy steels, *Journal of Alloys and Compounds* **451**, 534-537 (2008).
- [2] Heon Young Ha, Chan Jin Park, Hyuk Sang Kwon. Effect of misch metal on the formation of non-metallic inclusions in 25% Cr duplex stainless steels, *Scripta Materialia* **55**, 991-994 (2006).
- [3] M. Gajewski, J. Kasinska, Rare earth metals influence on mechanical properties and crack resistance of GP240GH and G17CrMo5-5 cast steels, *Archives of Foundry Engineering* **9**, 37-44 (2009).
- [4] K. Bolanowski, Structure and properties of MA-steel with rare earth elements addition, *Archives of Metallurgy and Materials* **50**, 327-332 (2005).
- [5] V.V. Luniov, Non metallic inclusions and properties of cast steels, *Foundry Journals of the Polish Foundrymen's Association* **53**, 9, 299-304 (2003) (in Polish).
- [6] J. Kasinska, Wide-ranging influence of mischmetal on properties of G17CrMo5-5 cast steel, *Metallurgija* **54**, 1, 135-138 (2015).
- [7] F.A. McClintok, A criterion for ductile fracture by growth of holes, *Journal of Applied Mechanics* **35**(4), 353-371 (1968).
- [8] F.A. Beremin, A local criterion for cleavage fracture of a nuclear pressure vessel steel, *Metallurgical Transaction A* **14A**, 2277-2287 (1983).
- [9] A. Seweryn, Brittle Fracture criterion for structures with sharp notches, *Engineering Fracture Mechanics* **45**(5), 673-681 (1994).
- [10] R.O. Ritchie, J.F. Knott, J.R. Rice, On the relationship between critical tensile stress and fracture toughness in mild steel, *Journal of the Mechanics and Physics of Solids* **21**, 395-410 (1973).
- [11] J.F. Knott, *Micromechanisms of fracture and fracture toughness of engineering alloys*, ICF-4 Fracture 1977 Waterloo, Canada **1**, 61-91 (1977).

- [12] A. Neimitz, J. Galkiewicz, I. Dzioba, The ductile to cleavage transition in ferritic Cr-Mo-V steel: A detailed microscopic and numerical analysis, *Engineering Fracture Mechanics* **77**, 2504-2526 (2010).
- [13] I. Dzioba, The influence of the microstructural components on fracture toughness of 13HMF steel, *Materials Science*, **47** (5), 357-364 (2011).
- [14] ASTM E1737-96. Standard Test Method for *J*-Integral Characterization of Fracture Toughness.
- [15] ASTM E1820-09. Standard Test Method for Measurement of Fracture Toughness, Annual book of ASTM standards **03.01**, 1070-1118 (2011).
- [16] ASTM E1921-10. Standard Test Method for Determination of Reference Temperature, T_0 , for Ferritic Steels in the Transition Range, Annual book of ASTM standards **03.01**, 1177-1198, (2011).
- [17] I. Dzioba, P. Furmanczyk, J. Kasinska, Fractographic study of G17CrMo5-5 cast steel fracture in a transition brittle-ductile region. XLIII School of Materials Engineering, ed. by J. Pacyna, AGH, Krakow-Rytko, 27-30.09.2015, 65-68 (in Polish).
- [18] C. Berdin, Damage evolution laws and fracture criteria. In *Local Approach to Fracture*, ed. by J. Besson, Paris, 147-174 (2004).
- [19] A. Neimitz, I. Dzioba, The influence of the out-of- and in-plane constraint on fracture toughness of high strength steel in the ductile to brittle transition temperature range, *Engineering Fracture Mechanics* **147**(10), 431-448 (2015).
- [20] J.R. Rice, D.M. Tracey, On the ductile enlargement of voids in triaxial stress fields, *Journal of the Mechanics and Physics of Solids* **17**, 201-217 (1969).
- [21] W. Guo, Elastoplastic three dimensional crack border field – I. Singular structure of the field, *Engineering Fracture Mechanics* **46**, 93-104 (1993).